GSI

GSI-95-22
PREPRINT
MAERZ 1995

TRACK STRUCTURE AND THE CALCULATION OF BIOLOGICAL EFFECTS OF HEAVY CHARGED PARTICLES

M. SCHOLZ, G. KRAFT

(To be published in 'Advances in Space Research')

Gesellschaft für Schwerionenforschung mbH
Postfach 110552 · D-64220 Darmstadt · Germany

Track Structure and the Calculation of Biological Effects of Heavy Charged Particles

M. Scholz and G. Kraft

GSI, Planckstrasse 1, D-64291 Darmstadt, FRG

ABSTRACT

A new approach for the calculation of biological effects of heavy charged particles is discussed. In contrast to other models, the biological effect is determined *locally* as a function of the local dose deposited by the charged particle tracks. Based on measurable quantities like the X-ray survival curve, the radial dose profile within a track and a geometrical description of the cell nucleus, the model is able to predict several high LET specific properties of charge particle beams, like

- the relationship of inactivation cross sections vs. LET and vs. specific energy;
- the RBE as a function of energy and atomic number of the particles, including the Z-dependent shift of RBE-maxima from 30 $keV/\mu m$ for protons to 300 $keV/\mu m$ for carbon ions;
- the transition from exponential to shouldered survival curves, depending on the size of the biological object and the corresponding particle fluences.

INTRODUCTION

The different spatial energy deposition pattern is the most obvious difference which can explain the enhanced RBE of charged particle beams compared to photon fields. Mainly two different approaches have been developed to model the biological effects of charged particles on the basis of their specific energy deposition pattern:

1. the microdosimetric approach, which emphasizes the stochastics of energy distribution on the basis of single electrons;
2. the 'amorphous' track structure approach, which is based on the radial dose distribution as a continous distribution, representing an average over many tracks.

The second approach has been shown to be most successful in describing and predicting biological effects as a function of the particle energy and atomic number /1,2,3,4/. However, in the case of extended targets, e.g. cell nuclei of mammalian cells, the calculation of biological effects in these models is based on the integration of the total energy deposited in the critical target. Due to this integration, corresponding to an averaging of the dose, the fine structure of the radial dose distribution is blurred. Therefore, we proposed a modified approach /5,6/, which is based on the *local* determination of the biological effect, thus reflecting even the fine structure of local dose depositions in the nucleus. In the previous papers we have described the general principles of the model calculations. This paper summarizes these basic principles and includes a more detailed comparison with experimental results.

LOCAL DOSE VS. AVERAGE OR TOTAL DOSE

The track structure model discussed here is based on the assumption that the biological effect is entirely determined by the spatial local dose distribution inside the cell nucleus, and that there is no principal difference between the action of local dose depositions of X-rays and charged particles. In sharp contrast to the energy deposition of X-rays, however, the dose distribution of charged particles is completely inhomogenous according the radial dose profile within the track, which roughly follows a $1/r^2$-law. The models of Katz and Kiefer perform an integration of the total energy deposited in the sensitive target, and the biological effect is read from the X-ray effect curve at the corresponding dose level. Here, the size of the critical target, which is in the order of some μm, plays a crucial role, because the integration of energy over a volume of μm-dimensions completely blurrs the fine structure of the local energy deposition pattern.

In particular, this step is critical if the X-ray effect curve is non-linear and exhibits a shoulder. The increasing slope of the shouldered curve implies, that high doses are relatively more efficient than low doses. If the same is valid for *local* doses as well, a certain energy deposited as a high local dose in a small subvolume of the nucleus should be more efficient compared to the same energy deposited as a low local dose in a larger subvolume. Therefore, integration of the energy and thus averaging over the nuclear volume will underestimate the biological effects produced by the high *local* doses in the center of a particle track.

According to these considerations, the biological effect has to be determined *locally*, which requires some knowledge about the distribution of sensitive sites in the cell. There is general agreement, that the cell nucleus is the critical target for inactivation, although there is a controversary, whether sensitive sites are distributed uniformly throughout the nucleus or whether they are located near the nuclear membrane. From their work with short range electrons and α-particles, Datta et al. /7/ conclude that sensitive sites are concentrated in the peripheral region of the cell nucleus. In contrast, the works of Lloyd et al. /8/ and Barendsen /9/ favour the hypothesis of a homogenous distribution of sensitive sites. This hypothesis is based on the observation that the biological effect depends only on the total length of tracks traversing the nucleus and is independent of the cell geometry. If only the number of membrane traversals were crucial, cell geometry should strongly influence the dose effect curves. Here, we will follow the arguments of Barendsen and others and assume a homogenous distribution of sensitive sites in the cell nucleus.

Besides the distribution of sensitive sites, the interaction of damages produced at different sites may influence the biological effect. Experiments performed with ultrasoft X-rays indicate that interaction distances must be on a scale in the order of some nm /10,11/. Because this distance is small compared to the size of the nucleus and the extension of the radial dose profile, we assume in a first approximation, that inactivation is the result of a point-like event (a 'lethal event'), which is completely determined by the local dose deposited either by X-rays or charged particles.

After X-irradiation, the average number of lethal events N depends on the dose D. The fraction of surviving cells can then be attributed to the cells, which actually carry *no* lethal event. Assuming that the distribution of lethal events obeys Poisson statistics, this can be written

$$S(D) = e^{-N(D)} \tag{1}$$

Vice versa, the number of lethal events can be derived from the X-ray survival curve as

$$N(D) = -ln\, S(D) \tag{2}$$

In the framework of the linear-quadratic model, for example, N(D) can be written as

$$N(D) = \alpha D + \beta D^2 \tag{3}$$

Due to the homogenous distribution of sensitive sites in the nucleus, lethal events will be randomly distributed throughout the nuclear volume V, and the event density

$$\nu(D) = \frac{N(D)}{V} = \frac{-ln\, S(D)}{V} \tag{4}$$

is constant within the nucleus. Equation (4) allows an easy calculation of survival in the case of partially irradiated nuclei or inhomogenous dose distributions. If only a part ΔV of the nucleus is irradiated with dose D, the average number of lethal events will be

$$\overline{N_{lethal}} = N(D)\frac{\Delta V}{V} \tag{5}$$

and in the case of an inhomogenous dose distribution, D(x,y,z), dependent on the position in the nucleus, $\overline{N_{lethal}}$ is obtained by an integration over the nuclear volume:

$$\overline{N_{lethal}} = \int_x \int_y \int_z \nu(D(x,y,z))\,dxdydz = \int_x \int_y \int_z \frac{-ln\,S(D(x,y,z))}{V}\,dxdydz \tag{6}$$

As in eq. 1, the fraction of surviving cells is given by the cells carrying no lethal event, and thus survival is calculated to be

$$S = e^{-\overline{N_{lethal}}} \tag{7}$$

Transition from Shouldered to Exponential Survival Curves

Due to the nonlinearity of the X-ray survival curve, the number of lethal events induced by the sum of two dose contributions is greater than the sum of lethal events for each single dose deposition:

$$N(D_1 + D_2) > N(D_1) + N(D_2) \tag{8}$$

The same is expected to be valid in the case of local doses, so that the efficiency of particles is increased compared to single tracks, if there is an overlap of their local dose distributions. Therefore, the biological effect has to be determined from the *total* local dose at a given point, summing up local doses from all particles contributing to a specific position in the cell nucleus.
According to these considerations, shouldered survival curves after charged particle irradiation can only be expected, if the track diameters and particle fluences are sufficiently large in order to obtain a significant fraction of energy deposited by superposition of local doses from several tracks. Conversely, there are two possible conditions leading to purely exponential survival curves:

- for very high LET particles, where the fluences are low and the fraction of energy deposited in overlap regions is negligible;
- for lower LET particles, if the energy is low, so that track diameters become small, and even for very high fluences there is only a small probability for different tracks to overlap.

As a consequence, even low energetic protons should exhibit an exponential survival curve, despite their comparably low LET and the high fluences used for inactivation experiments.

INPUT FROM EXPERIMENTAL DATA

As can be seen from eq. 6, three sets of experimental data will be required for the prediction of survival after charged particle irradiation:

1. the local dose distribution D(x,y,z), which is defined by the radial dose distribution D(r) inside the particle track and the position of particle trajectories;
2. the geometrical description of the cell nucleus, defining the sensitive volume V;
3. the X-ray survival curve S(D), which is used to derive the average number of lethal events N(D) and the event density $\nu(D) = \frac{N(D)}{V}$.

In the following, the basic assumptions used for the calculations will be briefly described and discussed.

Radial Dose Distributions

Although no direct measurements of D(r) have been performed in dense materials like water, the experiments using gas chambers /12,13/ as well as numerical calculations /1,14,15/ and Monte Carlo calculations /16/ suggest a $1/r^2$-dependence for the radial dose distribution. In order to avoid infinite values of D(r), a constant dose has been assumed for small radii below r_{min}=0.01 μm, so that D(r) can be described as

$$D(r) = \begin{cases} \lambda\ LET/r_{min}^2 & : \quad r < r_{min} \\ \lambda\ LET/r^2 & : \quad r_{min} \leq r \leq r_{max} \\ 0 & : \quad r > r_{max} \end{cases} \tag{9}$$

λ is a normalization constant, which is adjusted so that the integral over the whole track yields the LET as given by the tables of Hubert et al. /17/ and Northcliffe and Schilling /18/. The track radius r_{max} is determined by the range of the highest energetic electrons produced by the primary particle. Since the maximal electron energy depends on the specific energy E of the incoming particle, a function of the form

$$r_{max} = \gamma E^{\delta} \tag{10}$$

$$\gamma = 0.05; \delta = 1.7$$

has been used to describe the track radius, which results in similar values to those given in /14/ for energies between 1 and 20 MeV/u.

Geometrical structure of the critical targets

The shape of cell nuclei is assumed to be cylindrical with geometrical cross section A_{Nucl} and height H_{Nucl}. The particle trajectories are choosen parallel to the cylinder axis. Although radiosensitivity depends on the cell cycle stage and the size of cell nuclei increases with cell age, in a first approximation a unique radiosensitivity and size for all cells has been assumed in order to demonstrate the specific advantages of the model described below.

Care has to be taken when choosing the appropriate value representing the average size of the cells. As Todd and coworkers /19/ have pointed out, an effective geometrical nuclear cross section has to be used to represent a size distribution, which is in general smaller than the arithmetic mean value of the size distribution. If, for example, the frequency distribution for the size values is given by $h(\sigma)$, the probability not to be hit by any particle at a given particle fluence F is determined by

$$P(0) = \sum_{i=1}^{n} h(\sigma_i) \exp^{-\sigma_i F} \tag{11}$$

Due to the exponential weighting in eq. (11), small sizes have a higher weight than large sizes. Therefore, the effective cross section describing the hit probability can be considerably smaller than the average size. For example, for asynchronous Chinese hamster cells, we measured an average nuclear size of 75 μm^2, but an effective size of only 50 μm^2 /20/.

X-ray survival curves

In general, survival curves for mammalian cells show a shoulder for low doses and a purely exponential tail for higher doses. Although in principal the calculations are not restricted to a specific shape of the survival curve, we will focus on these shouldered survival curves.
We choose a parametrization which is linear quadratic for low doses and linear for high doses, thus combining the possible non-zero initial slope of the linear-quadratic model with the exponential tail of the multitarget/multihit formulation. In order to avoid confusion with the implications of the standard linear-quadratic formulation, coefficients for the linear and quadratic terms are called

a and b, respectively. The dose threshold D_t marks the transition from the shouldered to the exponential part of the survival curve. The slope of the survival curve at D=D_t is given according to the linear quadratic term to be

$$s = a + 2bD_t \tag{12}$$

Thus, survival is described in general by a function of the type

$$S(D) = \begin{cases} \exp(-aD - bD^2) & : \quad D \leq D_t \\ S_t \exp(-s(D - D_t)) & : \quad D > D_t \end{cases} \tag{13}$$

where S_t is the survival at the threshold dose D_t.

RESULTS AND DISCUSSION

In Fig. 1, model calculations for protons and α-particles are compared with experimental results taken from the literature. In Fig. 1a, X-ray survival curves as well as survival after irradiation with low energetic protons are shown. Whereas the agreement of calculations with the data of Folkard et al. is good, deviations from the data of Belli et al. are on the order of 25%. It has to be noted that differences in the experimental X-ray as well as in the proton survival curves are observed, although V79 cells were used in both cases. Since model predictions critically depend on the final slope of X-ray survival curves, but measurments are performed only down to the 10%-5% level, considerable uncertainties are expected. Survival curves after low energetic protons are exponential, as expected from the considerations discussed above. It should be noted that although exponential survival curves are often attributed to 1-hit mechanisms, an average number of 10 proton traversals is required to reduce survival to the 37% level. Comparison for α-particles shows (Fig. 1b), that there is a slight underestimation at the lowest energy, but for higher energies reasonable agreement is observed.

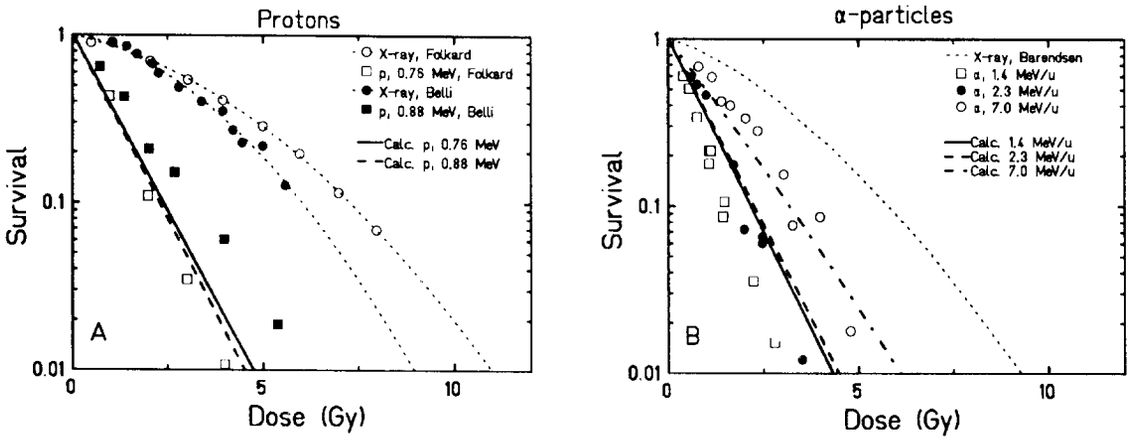

Figure 1: Comparison of calculated survival curves with experimental results. A: Irradiation of V79 Chinese hamster cells with low energetic protons. Experimental data redrawn from /21,22/. Input values for model calculation: A_{nucl} = 50μm^2, a=0.109, b=0.0283, D_t=17 Gy (Folkard et al.) a=0.136, b=0.0421, D_t=12 Gy (Belli et al.) B: Irradiation of T1 cells with α-particles. Experimental data redrawn from /23/. (A_{nucl} = 90μm^2, a=0.255, b=0.0263, D_t=20 Gy)

In order to facilitate the comparison of model calculations and experimental results, inactivation cross sections σ_{inact} were determined from the final slope of survival curves and plotted versus LET (Fig. 2). Although inactivation cross sections are slightly overestimated in the in the LET region around 20-50 $keV/\mu m$ and slightly underestimated around 200-300 $keV/\mu m$, the general structure of the σ-LET-dependence is predicted reasonably well by the model.

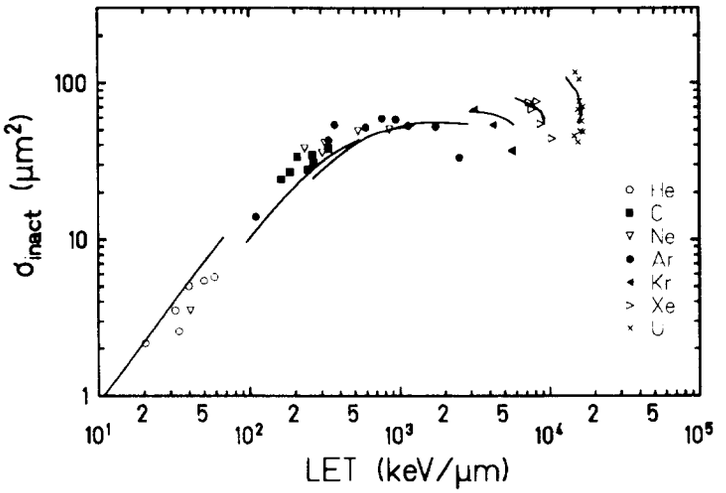

Figure 2: Comparison of model calculations for inactivation cross sections $\sigma_{inactivation}$ (full lines) with experimental results (symbols, redrawn from /24/), obtained with V79 Chinese hamster cells ($A_{nucl} = 50\mu m^2$, a=0.136, b=0.040, D_t=12 Gy)

The key to the understanding of the complex hook structure at very high LET is depicted in Fig. 3, where inactivation cross sections are plotted as a function of the energy per atomic mass unit for three representative ion species. At low velocities, all ions exhibit the same efficiency. The inactivation cross section is calculated to be $50\mu m^2$, which is equal to the effective geometrical size of the nucleus. Thus, a single traversal of any of the ions is sufficient to kill the cell with a high probability. With increasing energy, changes in LET as well as increasing track diameters are reflected in the σ-E-dependence.

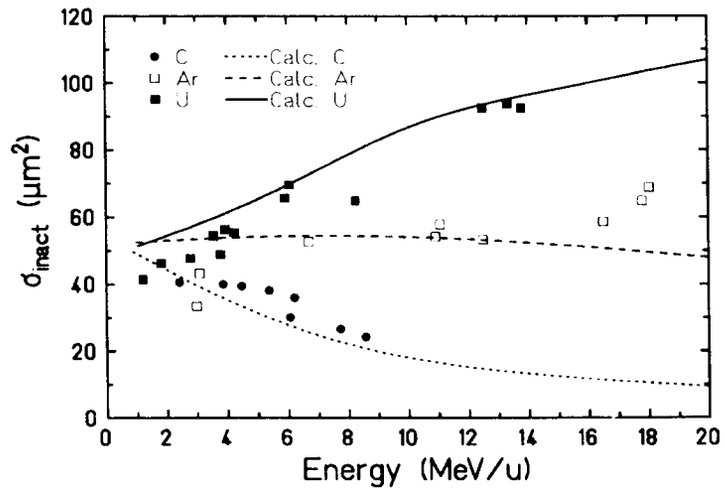

Figure 3: Inactivation cross sections for V79 cells as function of the specific energy for carbon, argon and uranium ions. Full lines: model calculations, symbols: experimental data (partially redrawn from /24/).

For uranium ions, there is only a slight decrease of LET in the energy range shown in Fig. 3, but there is a significant increase of the track radius according to eq. 10. Because of the very high LET, even at large distances from the trajectory high local doses are deposited. Therefore, not only direct traversals of the nucleus, but also traversals in a certain distance can inactivate the cell. The probability of these 'indirect' inactivation events increases with the track diameter, resulting in the rising inactivation cross section. For argon ions, there is a significant decline of LET from 3000 to

800 $keV/\mu m$ in the energy range from 1 to 20 MeV/u, and although the increase of the track radius is exactly the same as for the uranium ions, inactivation cross sections stay nearly constant over the whole energy range. This is a consequence of the much lower local doses at large distances from the track center, so that inactivation by a particle traversal outside the nucleus is very unlikely. In contrast, only the high local doses in the center of the track have a high probability to kill the cell, and thus *direct* traversals are required at all energies for the inactivation of a cell. For carbon ions, the decreasing LET dominates the σ-E-dependence. Now, only low energetic particles deposit high local doses sufficient to kill the cell by a single traversal. As a consequence of the decreasing LET with increasing specific energy, the energy deposition per particle traversal and thus the probability for inactivation decreases as well.

However, even for the light particles, the inactivation probability is not uniquely defined by their average energy deposition. Although the local doses at large distances are comparably small and inactivation by particle traversals outside the nucleus is unlikely, track structure still plays a critical role for the efficiency of particles. This is demonstrated in Fig. 4, where calculated RBE for protons, α-particles and carbon ions are compared. Obviously, RBE values cannot be described as a unique function of LET, but different, Z-dependent branches are predicted, resulting in different positions of RBE maxima. Whereas for protons the maximum is expected at 30 $keV/\mu m$, the maximum is shifted to $\approx$ 90 $keV/\mu m$ for α-particles and to $\approx$ 300 $keV/\mu m$ for carbon ions. These values coincide with the values reported e.g. by Belli et al. /22/, Thacker et al. /25/ and Kraft and Kraft-Weyrather /26/. As demonstrated in Fig. 4, lighter particles are predicted to be more efficient compared to heavier particles at the same LET. This is a result of the lower velocity of the lighter particle and the corresponding smaller track radius. As a consequence, the energy deposition is more concentrated at low velocities, whereas according to the $1/r^2$-distribution, the heavier particle deposits a larger fraction of energy as a low local dose in a greater distance from the particle trajectory. Therefore, the efficiency of the high velocity particles is reduced relative to the low velocity particles at the same LET.

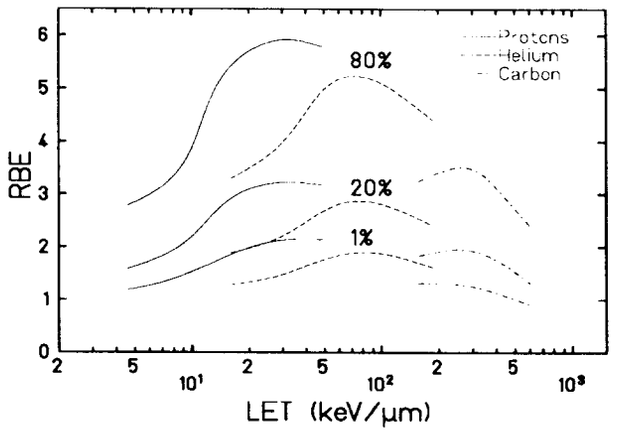

Figure 4: Model predictions for RBE as function of LET for protons, α-particles and carbon ions in the energy range from 1-20 MeV/u. (Calculations based on X-ray sensitivity and size as given in Fig. 2)

The decrease of RBE for carbon ions towards high LET values can be attributed to saturation effects due to cellular overkill mechanisms, which are also reflected in the transition to a plateau region of the σ-LET curve for LET greater than 300 $keV/\mu m$. As the saturation cross section coincides with the effective geometrical size of the nuclei, it can be attributed to the overkill effect, i.e. a single particle traversal is sufficient to kill the cell with a high probability. Differences between saturation cross sections and nuclear size, which have been reported earlier /24,27/, can be probably attributed at least partially to the differences between average and effective cross sections, as discussed in the subsection 'Geometrical structure of the critical targets'.

The correlation between overlap of tracks and shouldered survival curves, as predicted according to eq. 8 is schematically demonstrated in Fig. 5. Here, hypothetical survival curves for mammalian cells and yeast cells are compared for a 1 MeV/u and 5 MeV/u particle beam at 500 $keV/\mu m$. Mammalian cells as well as yeast cells are assumed to exhibit the same shape of X-ray survival curve, i.e. the same shoulder width and the same ratio of final to initial slope. For mammalian cells, survival curves for b 'h 1 MeV/u and 5 MeV/u are predicted to be purely exponenti:!, although the 5 MeV/u particles are somewhat less efficient. In contrast, for yeast cells only at 1 MeV/u exponential survival is seen, whereas for 5 MeV/u already a significant shoulder is expected.

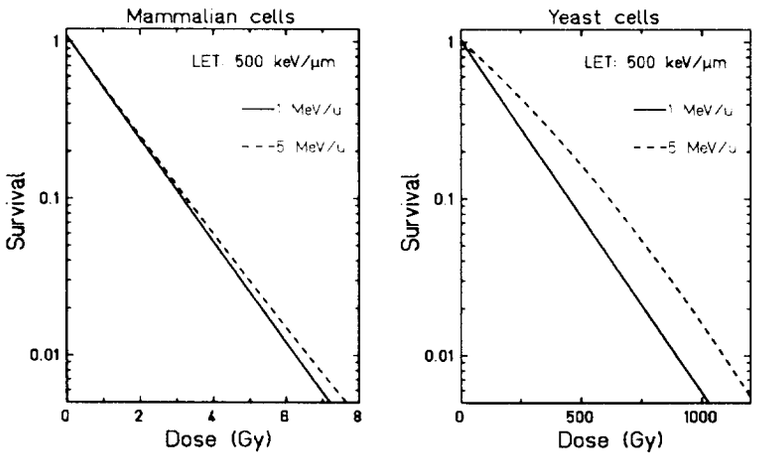

Figure 5: Differences in the transition from exponential to shouldered survival curves as predicted by the model for different biological objects. Calculations based on hypothetical X-ray survival curves and particles with an LET of 500 $keV/\mu m$. Mammalian cells: $A_{nucl} = 50\mu m^2$, a=0.02, b=0.05, D_t=12 Gy Yeast cells: $A_{nucl} = 0.5\mu m^2$, a=1e-4, b=1e-6, D_t=600 Gy

These differences can be interpreted in terms of track radii and particle fluences and the corresponding overlap of tracks. In order to end up at a similar survival level, the particle fluences used for irradiation of yeast cells have to be roughly 100 times higher compared to the fluences used for mammalian cells. At low energies, where the track radius is small, even at the high fluence there is only a minor probability for the superposition of different tracks. At the higher energy and the correspondingly large track diameters, there is a very high probability for superposition of several tracks, whereas at the low fluences it is still very unlikely to have significant fractions of energy deposited by overlapping tracks. Experimental results obtained with yeast cells, showing shouldered survival curves even after irradiation with heavier ions like argon and krypton support the considerations discussed above /28/.

CONCLUSIONS

As has been demonstrated in this paper, several high LET specific radiobiologic properties of charged particle beams can be put down to their specific spatial energy deposition pattern. As the most significant difference to other similar models, the approach discussed here is based on the determination of the *local* biological effect even in the case of extended targets like e.g. nuclei of mammalian cells. In contrast to other models, the prediction of survival probabilities is entirely based on measurable quantities, and no free parameters are introduced. As a consequence, exactly the same algorithm can be used for the calculations over the whole LET range from 2-15000 $keV/\mu m$. This is a specific advantage compared to the Katz model, where two independent modes of inactivation have to be introduced explicitly, which dominate at low LET and high LET, respectively.

The determination of *local* biological effects is in particular crucial in the case of light particles with inactivation cross sections below the saturation level reached at $\approx 300\ keV/\mu m$. For example, for low energetic protons, the average dose deposited per particle traversal in the nucleus is very small. Calculation of the biological effect based on the *average* dose would thus predict a low efficiency, whereas only the prediction based on the high *local* dose is able to predict correctly the high RBE observed in experiments.

Although the model is still based on certain simplifications, a reasonable agreement between model predictions and experimental results is already achieved. The remaining differences are expected to be diminished in future developments of the model, which will focus on a more detailed description of the input data. For example, the cell-cycle dependent radiosensitivity, which is expressed as a significant variation of the shape of X-ray survival curves for cells in different cycle stages, will be taken into account. Since the prediction of RBE critically depends on the shoulder shape of the X-ray survival curve, the most detailed information available should be put in the model calculations. Similarly, the cell-cycle dependent nuclear size and geometry will be taken into account.

REFERENCES

1. Butts, J.J. and Katz, R., 1967, Theory of RBE for heavy ion bombardment of dry enzymes and viruses. *Radiation Research*, **30**, 855-879
2. Katz, R., Ackerson, B., Homayoonfar, M. and Sharma, S.C., 1971, Inactivation of cells by heavy ion bombardment. *Radiation Research*, **47**, 402-425
3. Katz, R., Dunn, D.E. and Sinclair, G.L., 1985, Thindown in radiobiology. *Radiation Protection Dosimetry*, **13**, 281-284
4. Kiefer, J., 1982, On the interpretation of heavy ion survival data. Proc. of the 8th Symposium on Microdosimetry, eds. Booz, J. and Ebert, H.G., 729-742
5. Scholz, M., and Kraft, G., 1992, A parameter free track structure model for heavy ion action cross sections. In: Biophysical Modelling of Radiation Effects. Edited by: K.H. Chadwick, G. Moschini and M.N. Varma (Adam Hilger, Bristol), 185-192
6. Scholz, M., and Kraft, G., 1994, Calculation of heavy ion inactivation probabilities based on track structure, X-ray sensitivity and target size, *Radiation Protection Dosimetry*, **52**, 29-33
7. Datta, R., Cole, A. and Robinson, S., 1976, Use of track-end slpha particles from ^{241}Am to study radiosensitive sites in CHO cells, *Radiation Research*, **65**, 139-151
8. Lloyd, E.L., Gemmell, M.A., Henning, C.B., Gemmell, D.S., and Zabransky, B.J., 1979, Cell survival following multiple-track alpha particle irradiation, *Radiation Research*, **35**, 23-31
9. Barendsen, G.W., 1990, LET dependence of linear and quadratic terms in dose-response relationships for cellular damage: correlations with the dimensions and structures of biological targets, *Radiation Protection Dosimetry*, **31**, 235-239
10. Cox, R., Thacker, J., and Goodhead, D.T., 1977, Inactivation and mutation of cultured mammalian cells by aluminium characteristic ultrasoft X-rays. III.Dose-response of Chinese hamster and human diploid cells to aluminium X-rays and radiations of different LET. *International Journal of Radiation Biology***31**, 561-576
11. Goodhead, D.T., Thacker, J., and Cox, R., 1979, Effectiveness of 0.3 keV carbon ultrasoft X-rays for the inactivation and and mutation of cultured mammalian cells. *International Journal of Radiation Biology*, **36**, 101-114
12. Varma, M.N., Baum, J.W. and Kuehner, A.V., 1977, Radial dose, LET and $\overline{W}$ for ^{16}O ions in N_2 and tissue-equivalent gases. *Radiation Research*, **70**, 511-518
13. Metting, N.F., Rossi, H.H., Braby, L.A., Kliauga, P.J., Howard, J., Zaider, M., Schimmerling, W., Wong, M. and Rapkin, M., 1988, Microdosimetry near the trajectory of high energy ions. *Radiation Research*, **116**, 183-195
14. Chatterjee, A. and Magee, J.L., 1980, Energy transfer from heavy particles. In: Biological and medical research with accelerated heavy ons at the BEVALAC 1977-1980, eds. M.C. Pirucello and C.A. Tobias, LBL-report 11220 (University of California, Berkeley), 55-61

15. Kiefer, J. and Straaten, H., 1986. A model of ion track structure based on classical collision dynamics. *Physics in Medicine and Biology*, **31**, 1201-1209

16. Krämer, M. and Kraft, G., 1994, Calculations of heavy-ion track structure, *Radiation and Environmental Biophysics*, **33**, 91-109

17. Hubert, F., Fleury, A., Bimbot, R. and Gardes, D., 1980, Range and Stopping Power Tables for 2.-100 MeV/Nucleon Heavy Ions in Solids, Ann. Phys. Suppl. **5**, 1-214

18. Northcliff L.C. and Shilling, R.F., 1970, Range and stopping power tables for heavy ions, Nucl. Data Tables **A7**, 233-437

19. Todd, P., Wood, J.C.S., Walker, J.T. and Weiss, S.J., 1985, Lethal, potential lethal, and nonlethal damage induction by heavy ions in cultured human cells, *Radiation Research*, **104**, S5-S12

20. Scholz, M., 1992, Zellzyklusverzögerungen synchroner Zellpopulationen nach Schwerionenbestrahlung, Thesis, GSI-Report 92-28

21. Folkard, M., Prise, K.M., Vojnovic, B., Davies, S., Roper, M.J. and Michael, B.D., 1989, The irradiation of V79 mammalian cells by protons with energies below 2 MeV. Part I: Experimental arrangement and measurements of cell survival. *International Journal of Radiation Biology*, **56**, 221-237

22. Belli, M., Cera, F., Cherubini, R., Haque, A.M.I., Ianzini, F., Moschini, G., Sapora, O., Simone, G., Tabocchini, M.A. and Tiveron, P., 1993, Inactivation and mutation induction in V79 cells by low energy protons: re-evaluation of the results at the LNL facility, *International Journal of Radiation Biology*, **63**, 331-337

23. Barendsen, G.W., Walter, H.M.D., Fowler, J.F. and Bewley, D.K., 1963, Effects of different ionizing radiations on on human cells in tissue culture. III: Experiments with cyclotron-accelerated alpha-particles and deuterons *Radiation Research*, **18**, 106-119

24. Kraft, G., 1987, Radiobiological effects of very heavy ions: inactivation, induction of chromosome aberrations and strand breaks. *Nuclear Science Applications*, **3**, 1-28

25. Thacker, J., Stretch, A. and Stephens M.A., 1979, Mutation and inactivation of cultured mammalian cells exposed to beams of accelerated heavy ions. *International Journal of Radiation Biology*, **36**, 137-148

26. Kraft, G. and Kraft-Weyrather, W., 1987, Biophysical aspects of track structure, Proc. of the 8th ICRR (Edinburgh), Vol. 2, 29-34

27. Wulf, H., Kraft-Weyrather, W., Miltenburger, H.G., Blakely, E.A., Tobias, C.A. and Kraft, G., 1985, Heavy-ion effects on mammalian cells: inactivation measurements with different cell lines. *Radiation Research*, **104**, S122-S134

28. Schöpfer, F., Schneider, E., Rase, S. and Kiefer, J., 1982, Heavy-ion effects on yeast: survival and recovery in vegetative cells of different sensitivity, *Radiation Research*, **92**, 30-46